Tipping the Scales: The Migration–Selection Balance Leans toward Selection in Snake Venoms

Mark J. Margres,*[†,1,2] Austin Patton,[2] Kenneth P. Wray,[1] Alyssa T.B. Hassinger,[‡,1] Micaiah J. Ward,[1] Emily Moriarty Lemmon,[1] Alan R. Lemmon,[3] and Darin R. Rokyta[1]

[1]Department of Biological Science, Florida State University, Tallahassee, FL

[2]School of Biological Sciences, Washington State University, Pullman, WA

[3]Department of Scientific Computing, Florida State University, Tallahassee, FL

[†]Present address: Department of Biological Sciences, Clemson University, Clemson, SC

[‡]Present address: Department of Evolution, Ecology, and Organismal Biology, Ohio State University, Columbus, OH

***Corresponding author:** E-mail: mmargre@clemson.edu.

Associate editor: Gregory Wray

Abstract

The migration–selection interaction is the strongest determinant of whether a beneficial allele increases in frequency within a population. Results of empirical studies examining the role of gene flow in an adaptive context, however, have largely been equivocal, with examples of opposing outcomes being repeatedly documented (e.g., local adaptation with high levels of gene flow vs. gene swamping). We compared neutral genomic and venom expression divergence for three sympatric pit vipers with differing ecologies to determine if and how migration–selection disequilibria result in local adaptation. We specifically tested whether neutral differentiation predicted phenotypic differentiation within an isolation-by-distance framework. The decoupling of neutral and phenotypic differentiation would indicate selection led to adaptive divergence irrespective of migration, whereas a significant relationship between neutral and venom expression differentiation would provide evidence in favor of the constraining force of gene flow. Neutral differentiation and geographic distance predicted phenotypic differentiation only in the generalist species, indicating that selection was the predominant mechanism in the migration–selection balance underlying adaptive venom evolution in both specialists. Dispersal is thought to be a stronger influence on genetic differentiation than specialization, but our results suggest the opposite. Greater specialization may lead to greater diversification rates, and extreme spatial and temporal variation in selective pressures can favor generalist phenotypes evolving under strong stabilizing selection. Our results are consistent with these expectations, suggesting that the equivocal findings of studies examining the role of gene flow in an adaptive context may be explained by ecological specialization theory.

Key words: **adaptation, expression, migration, ecology, venoms.**

Introduction

Gene flow is an evolutionary force affecting adaptation, speciation, and coevolution (among other processes) and has received substantial attention, particularly because local adaptive differentiation depends on the balance of gene flow and selection (Endler 1977; Slatkin 1987; Garant et al. 2007; Savolainen et al. 2013). The interaction between gene flow and selection is the strongest determinant of whether a beneficial allele increases in frequency within a population (Tigano and Friesen 2016), but how migration–selection disequilibria often result in local adaptation is unclear. Traditional theory described gene flow as a homogenizing force opposing directional selection and preventing local adaptation, particularly when the migration rate exceeded fitness differences across populations (Bulmer 1972; Endler 1977; Slatkin 1987; Garcia-Ramos and Kirkpatrick 1997).

Some early work, however, questioned whether gene flow always hindered local adaptation (Ehrlich and Raven 1969; Felsenstein 1977; Charlesworth et al. 1982). Slatkin (1976) suggested that the strength of selection, rather than migration rate, had the greatest effect on how quickly an advantageous allele spread across a metapopulation. More recent studies have shown that the interaction between gene flow and selection can be extremely complex (Garant et al. 2007; Nuismer and Gandon 2008). High levels of gene flow can disrupt local adaptation, but migration may also stimulate adaptive evolution in certain scenarios (Fitzpatrick et al. 2015), such as in inbred populations or coevolutionary interactions (Gandon and Nuismer 2009), by increasing genetic variation and, therefore, the range of phenotypes on which selection can act. Intermediate levels of gene flow have often been proposed to allow the greatest amount of adaptive divergence (Garant et al. 2007), and examples of local adaptation with high levels of gene flow have been repeatedly documented (Linnen et al. 2009; Muir et al. 2014; Pfeifer et al. 2018). Equivocal findings of studies examining the role of gene flow in an adaptive context demonstrate the complex nature of the migration–selection interaction and highlight

Article

the need for more empirical work to identify the specific conditions under which local adaptation occurs.

One such condition hypothesized to affect adaptive divergence is the degree of specialization (Futuyma and Moreno 1988). How ecological specialization influences diversity has been an active debate (reviewed in Devictor et al. 2010), and dispersal has often been thought to be a stronger influence on genetic differentiation than specialization. Several studies have directly compared neutral differentiation across sympatric specialists and generalists (Kelley et al. 2000; Packer et al. 2005; Groot et al. 2011), but, to our knowledge, such comparative studies have not focused on putatively adaptive phenotypic differentiation or the migration–selection balance in the context of ecological specialization theory (Futuyma and Moreno 1988).

Comparing rates of gene flow and patterns of adaptive divergence for multiple species across the same landscape, particularly species with different ecologies, has been labeled an important next step in our understanding of the migration–selection balance (Sexton et al. 2014). Comparative studies of sympatric species can help identify the processes driving patterns of phenotypic differentiation, and comparing trait distributions for independent lineages across the same landscape will show whether adaptive or neutral processes are responsible for the observed phenotypic variation (Garcia-Ramos and Kirkpatrick 1997; Lenormand 2002; Colosimo et al. 2005; Gomulkiewicz et al. 2007; Blanquart et al. 2013; Margres, et al. 2015). Trait differences among populations can be the result of selection, but demonstrating local adaptation requires fitness comparisons which are often difficult in many systems (reviewed in Savolainen et al. 2013) with a few noteworthy exceptions (Colosimo et al. 2005; Linnen et al. 2013; Martin and Wainwright 2013). In the absence of fitness data, comparing putatively adaptive variation in fitness-related traits to neutral genetic differentiation may enable the identification of locally adapted phenotypes (Blanquart et al. 2013; Savolainen et al. 2013; Margres et al. 2015). For example, phenotypic variation among populations that can be accounted for by neutral genomic divergence may be a result of genetic drift, but trait variation that exceeds neutral divergence is indicative of directional selection (Garcia-Ramos and Kirkpatrick 1997; Whitehead and Crawford 2006; Blanquart et al. 2013; Muir et al. 2014).

Here, we compared neutral genomic and venom expression differentiation across three sympatric pit vipers with differing ecologies in the southeastern United States, the eastern diamondback rattlesnake (*Crotalus adamanteus*), pygmy rattlesnake (*Sistrurus barbouri*), and cottonmouth (*Agkistrodon piscivorus*), to characterize the migration–selection balance and local, adaptive venom divergence. Recent work has indicated that prey-preference in venomous snakes is genetic (Holding et al. 2016). *Agkistrodon piscivorus* is a dietary generalist and opportunistic scavenger, with documented prey items including (but certainly not limited to) fish, arthropods, amphibians, reptiles, mammals, and mollusks (Kofron 1978; Vincent et al. 2004). *Sistrurus miliarius* most frequently consumes reptiles and frogs (~60%), with small mammals and centipedes representing minor dietary components (~30%; Roth et al. 1999; Gibbs and Mackessy 2009). *Crotalus adamanteus* is the most specialized of the three species, consuming mostly rodents (e.g., *Sigmodon hispidus* ~57% of the diet in north Florida) and lagomorphs, but will take the occasional bird (collated and reviewed in Means 2017).

Snake venoms are polygenic traits comprised of toxic proteins that collectively function in predation and defense (Boldrini-França et al. 2010; Calvete et al. 2010; Casewell et al. 2012) and have repeatedly been shown to evolve under strong selection (Daltry et al. 1996; Casewell et al. 2011; Margres et al. 2013; Vonk et al. 2013). Toxin expression levels often predict venom function (Sánchez et al. 2005; Margres et al. 2016), and relative amounts of venom components have been shown to underly local, adaptive differences in venom efficacy in natural prey (Holding, Biardi, et al. 2016; Margres et al. 2017). Because venom is a secretion, protein expression can be measured directly by reversed-phase high-performance liquid chromatography (RP-HPLC), and the individual proteins present in each RP-HPLC peak (i.e., transcriptome–proteome map) have previously been identified for each of the three focal species (Margres et al. 2016).

We used genomics and proteomics to quantify and compare neutral genomic and venom expression divergence for each species independently to determine if and how migration–selection disequilibria result in local adaptation in venoms. The decoupling of neutral genomic and venom expression differentiation would indicate a lack of a role for gene flow promoting or hindering adaptive divergence, whereas a significant relationship between neutral and venom expression differentiation would provide evidence in favor of gene flow's importance. We specifically tested whether 1) neutral differentiation predicted phenotypic differentiation, 2) geographic distance predicted neutral differentiation (neutral isolation-by-distance [IBD]), and 3) geographic distance predicted venom expression differentiation (trait IBD). Evidence for the first and/or third hypotheses would indicate gene flow was an important mechanism underlying and constraining venom expression differentiation, whereas evidence for alternative hypotheses would indicate the migration–selection balance tipped toward selection in snake venoms.

Results and Discussion

Characterizing Population Structure and Effective Migration Rates across the Landscape

To characterize the migration–selection balance in venoms, we first needed to quantify the level of neutral genetic differentiation within each species. We used a target capture approach and identified 6,781, 20,104, and 8,347 putatively neutral SNPs from across the genome in *C. adamanteus*, *S. miliarius*, and *A. piscivorus*, respectively. We then used this genomic information to identify population structure, quantify neutral genomic divergence, and estimate effective migration surfaces for each species (fig. 1).

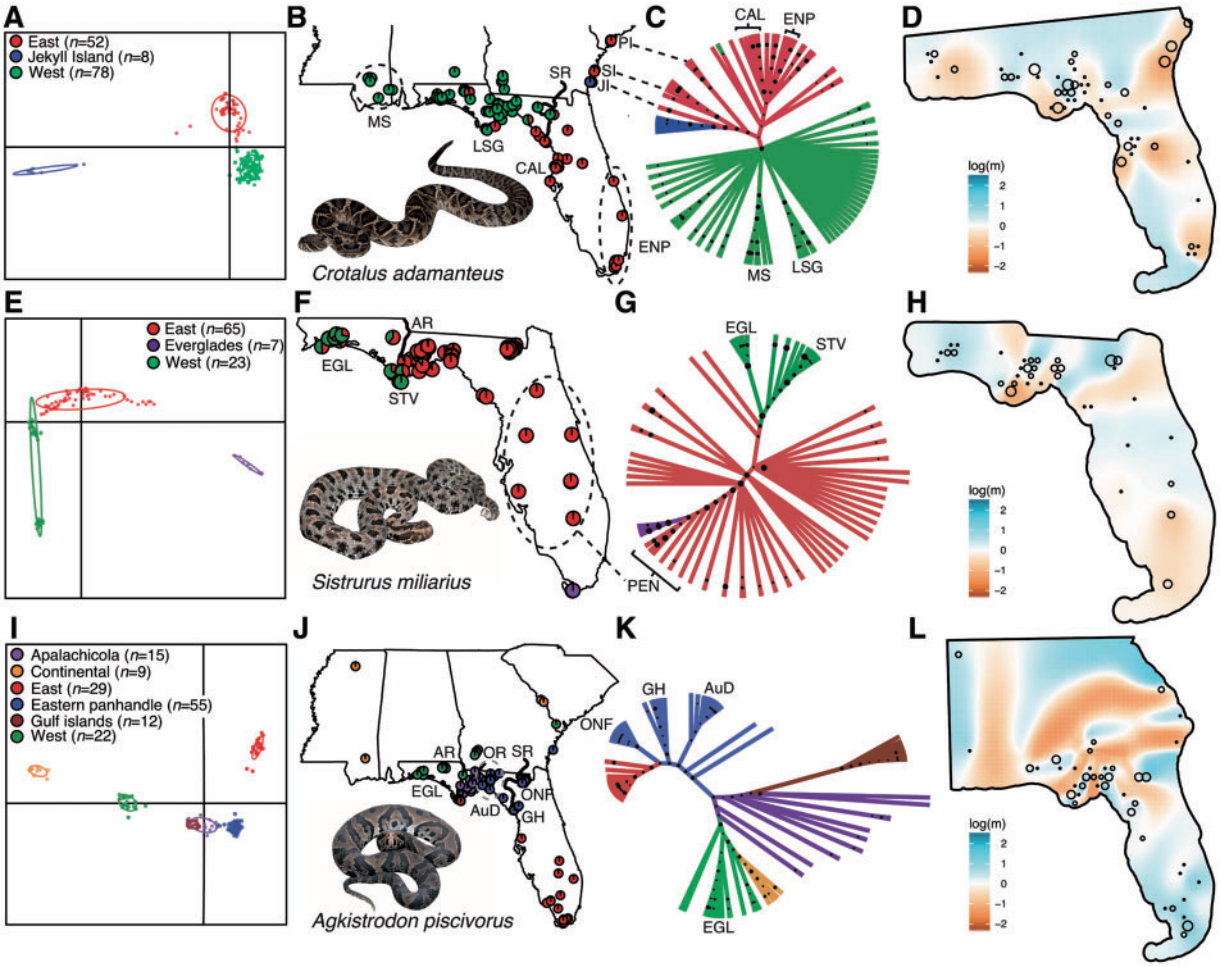

Fig. 1. Identifying population structure and estimating effective migration surfaces for *Crotalus adamanteus* (*A*–*D*), *Sistrurus miliarius* (*E*–*H*), and *Agkistrodon piscivorus* (*I*–*L*). A clustering algorithm with a discriminant analysis of principal components (DAPC) identified three, three, and six distinct genetic clusters across each species; scatter plots are shown in panels (*A*), (*E*), and (*I*), respectively. (*B*, *F*, and *J*) Mapping the distinct genetic clusters. The DAPC calculated membership probabilities for each individual for each cluster; pie charts on the map reflect the membership probability for each individual. Mixed pie charts suggest the presence of admixture, which was evident across the eastern and western clusters in *C. adamanteus* (*B*) and *S. miliarius* (*F*). (*C*, *G*, and *K*) Unrooted phylogenies for each species identified additional population structure. All monophyletic populations identified on the phylogeny are also labeled on the map. Node sizes are proportional to bootstrap support, and nodes with bootstrap support <0.25 were collapsed. Colors are consistent with previous panels. (*D*, *H*, and *L*) Estimated effective migration surfaces for each species. The heat map indicates estimated effective migration rates. Cooler colors represent higher effective migration rates, and warmer colors represent lower effective migration rates. Migration rates (m) are reported as migrants/generation on a log scale where $log(m) = 1$ represents a 10× greater effective migration rate than the average rate across the landscape. Points represent sampling locations with the size of the point proportional to sample size. Abbreviations: AR, Apalachicola River; AuD, Aucilla River Drainage; CAL, Caladesi Island; EGL, Eglin Air Force Base; ENP, Everglades National Park; GH, Gulf Hammock; JI, Jekyll Island; LSG, Little St George Island; MS, Mississippi; ONF, Osceola National Forest; OR, Ochlockonee River; PEN, Peninsular Florida; PI, Parris Island; SI, Sapelo Island; SR, Suwannee River; STV, St Vincent Island. Photo credit: Kenneth P. Wray.

A discriminant analysis of principal components (DAPC) identified three, three, and six distinct genetic clusters for *C. adamanteus*, *S. miliarius*, and *A. piscivorus*, respectively (fig. 1*A*, *B*, *E*, *F*, *I*, and *J*). Pairwise F_{ST} estimates ranged from 0.0200 to 0.0713 in *C. adamanteus* (supplementary table S1, Supplementary Material online), 0.0238–0.1519 in *S. miliarius* (supplementary table S2, Supplementary Material online), and 0.0328–0.2860 in *A. piscivorus* (supplementary table S3, Supplementary Material online). We performed hierarchical DAPC runs within these genetic clusters to potentially identify additional structure. We found weak evidence for additional structure within the eastern *C. adamanteus* cluster (supplementary fig. S1, Supplementary Material online), strong evidence for additional structure within the western *S. miliarius* cluster (supplementary fig. S2, Supplementary Material online), and strong evidence for additional structure within the *A. piscivorus* eastern panhandle cluster (supplementary fig. S3, Supplementary Material online).

To complement these assignment tests, we estimated an unrooted phylogeny in SVDquartets (Chifman and Kubatko 2014) for each species and again identified additional structure (fig. 1*C*, *G*, and *K*). For *C. adamanteus*, we identified monophyletic clades for two subpopulations within the western cluster and four subpopulations within the eastern cluster

Table 1. Mean, Untransformed Effective Migration Rates for Each DAPC Genetic Cluster.

DAPC Cluster	*Crotalus adamanteus*	*Sistrurus miliarius*	*Agkistrodon piscivorus*
East	4.673	0.583	2.567
West	4.844	0.583	2.568
Jekyll Island	4.507	—	—
Everglades	—	0.583	—
Apalachicola	—	—	2.572
Continental	—	—	2.584
Eastern panhandle	—	—	2.586
Gulf Islands	—	—	2.563

NOTE.—Effective migration rates represent the number of migrants per generation being exchanged between the specific DAPC cluster and neighboring demes. Mean rates were calculated by extracting the value at each individual sampling location and averaging across all individuals/DAPC genetic cluster.

(fig. 1C). For *S. miliarius*, we identified monophyletic clades for two subpopulations within the western cluster and for one subpopulation within the eastern cluster (fig. 1G). For *A. piscivorus*, we identified monophyletic clades for three subpopulations within the eastern panhandle cluster and for an additional subpopulation within the western cluster (fig. 1K); all subpopulations are labeled in figure 1, and phylogenetic analyses were largely consistent with the hierarchical DAPC results. Overall, we identified strong evidence for three populations and six subpopulations in *C. adamanteus*, three populations and three subpopulations in *S. miliarius*, and six populations and four subpopulations in *A. piscivorus*.

We next used EEMS (Petkova et al. 2016) to estimate spatially variable migration rates across the landscape for each species. EEMS results were largely consistent with the assignment tests and phylogenetic analyses described earlier (fig. 1D, H, and L). Particular topographical features, such as rivers, appeared to vary as to whether they reduced effective migration across all three species. For example, the Suwannee River, a known suture zone for continental and peninsular Florida lineages (Bert 1986), reduced effective migration in all three taxa, but more substantially in *C. adamanteus* and *S. miliarius* (fig. 1D, H, and L). Mean, untransformed effective migration rates are provided for each DAPC cluster in table 1. Because the underlying EEMS model assumes symmetric rates of migration, our metric represents the mean number of migrants per generation being exchanged between said population and all neighboring demes (Petkova et al. 2016).

Through assignment tests, *F* statistics, phylogenetic analyses, and effective migration surface estimations, we thoroughly quantified neutral differentiation across all three taxa.

Characterizing Venom Expression Differentiation across the Landscape

We next used the population structure identified above to guide our trait-based analyses characterizing the pattern of venom expression divergence for all three species under low-migration (using across DAPC cluster comparisons) and high-migration (using within DAPC cluster comparisons) regimes. We used RP-HPLC and the previously characterized transcriptome–proteome map for each species to quantify venom expression as previously described (Margres et al. 2016). Briefly, relative amounts of individual peaks were determined by measuring the area under each RP-HPLC peak relative to the total area of all identified peaks, and raw data were transformed using the isometric logratio transformation (ilr) as previously described (see Materials and Methods for details; Margres et al. 2014; Wray et al. 2015). We then used these data to quantify the frequency of the following four patterns: 1) low gene flow with significant evidence of phenotypic differentiation indicating drift or directional selection, 2) low gene flow without significant evidence of phenotypic divergence indicating strong stabilizing selection/lack of spatially varying selection, 3) greater gene flow with significant evidence of phenotypic divergence indicating strong directional selection, and 4) greater gene flow without significant evidence of phenotypic divergence indicating swamping and/or stabilizing/lack of spatially varying selection. Pattern 1 would indicate that gene flow may play a substantial role in enabling venom differentiation (i.e., gene flow is low enough to allow local adaptation or drift), pattern 2 would indicate that selection plays a larger role (i.e., despite gene flow being low enough to allow local adaptation, strong stabilizing selection/lack of spatially varying selection did not result in adaptive differentiation), pattern 3 (like 2) would indicate that the migration–selection balance leaned toward selection, and pattern 4 (like 1) would indicate that gene flow played a more substantial, and possibly deterministic, role in local adaptation in venoms.

We first used the identified DAPC clusters to characterize venom divergence across populations under low gene flow and quantify the frequency of patterns 1 and 2. We identified significant expression differentiation among DAPC genetic clusters across all three species ($0.001 < P < 0.043$). Significant ontogenetic expression differentiation was detected in *C. adamanteus* ($P < 0.001$) and *A. piscivorus* ($P = 0.004$), but not *S. miliarius* ($P = 0.173$). No interaction terms were significant ($0.252 < P < 0.804$). Because of the significant ontogenetic shift in venom expression, we restricted our pairwise comparisons to adults in all three taxa for consistency. Pairwise comparisons among the three *C. adamanteus* clusters revealed that all clusters were significantly different ($0.001 < P < 0.003$; supplementary fig. S4A, Supplementary Material online). Pairwise comparisons among the three *S. miliarius* clusters revealed that only the western cluster was significantly different ($P = 0.022$; supplementary fig. S5A, Supplementary Material online). In *A. piscivorus*, all pairwise comparisons among the six clusters were significant ($0.001 < P < 0.048$) except for four comparisons in the panhandle region of Florida ($0.118 < P < 0.324$), indicating a single venom phenotype across the four genetic clusters found in that region (supplementary fig. S6A, Supplementary Material online). Collectively, we identified significant variation in venom expression patterns across DAPC genetic clusters in all three species. We only found evidence of pattern 1 in *C. adamanteus* (all neutrally defined populations exhibit significantly different venoms). Although we found evidence of both patterns in *S. miliarius* (two expression phenotypes

across three genetic clusters) and *A. piscivorus* (three expression phenotypes across six genetic clusters), pattern 2 was more frequent.

We next used discrete sampling localities to characterize venom divergence under high gene flow (i.e., within each DAPC cluster) and quantify the frequency of patterns 3 and 4. For *C. adamanteus*, we compared four sampling localities within the eastern cluster and three sampling localities within the western cluster (supplementary fig. S4, Supplementary Material online). We detected significant expression differentiation among the eastern localities ($P < 0.0001$; supplementary fig. S4*B*, Supplementary Material online), and all sampling localities were significantly different ($0.001 < P < 0.008$). We did not identify significant expression differentiation among the western sampling localities in the full model ($P = 0.102$), although pairwise comparisons did identify significant differences between island and mainland sites ($0.042 < P < 0.048$; supplementary fig. S4*C*, Supplementary Material online), consistent with previous results (Margres et al. 2017). For *S. miliarius*, we compared two sampling localities within the western cluster and three sampling localities within the eastern cluster (supplementary fig. S5, Supplementary Material online). We detected significant expression differentiation among the eastern ($P = 0.008$; supplementary fig. S5*B*, Supplementary Material online) and western ($P = 0.001$; supplementary fig. S5*C*, Supplementary Material online) localities. Pairwise comparisons indicated that only the Apalachicola site was significantly different in the east ($0.009 < P < 0.028$). Because of the extensive population structure in *A. piscivorus*, our within-cluster analyses were limited to a single comparison of two sampling localities within the eastern panhandle cluster where we detected significant expression differentiation ($P = 0.031$; supplementary fig. S6*B*, Supplementary Material online). Here, pattern 3 (i.e., selection) was significantly more frequent than pattern 4 across all species (χ^2 goodness-of-fit, $P = 0.035$). Five of six, three of four, and a singular comparison found significant statistical evidence for the migration–selection interaction leaning toward selection (pattern 3) rather than gene flow (pattern 4) across all three species. Selection, therefore, appears to be the predominant mechanism driving local venom divergence in *C. adamanteus* and *S. miliarius*; the sample size in *A. piscivorus* was too low to identify a pattern. Because these comparisons of neutral and phenotypic patterns of differentiation were largely qualitative, we next directly compared neutral and venom expression divergence in a quantitative framework.

Characterizing the Migration–Selection Balance in Venoms

To quantitatively compare neutral and phenotypic differentiation, we constructed simple regression models (*lm* function in R) comparing neutral genetic differentiation (F_{ST}), venom phenotypic distance, and geographic distance across all populations/subpopulations for each of the three species (fig. 2). If the migration–selection interaction was more strongly influenced by migration, we would expect neutral differentiation to predict phenotypic differentiation and/or find evidence of trait IBD. If the migration–selection balance leaned toward selection, however, we would not expect a significant relationship between venom phenotypic distance and F_{ST}/geographic distance.

Neutral genetic differentiation was only a significant predictor of phenotypic differentiation in *A. piscivorus* ($P < 0.001$); neither *C. adamanteus* ($P = 0.196$) nor *S. miliarius* ($P = 0.792$) exhibited a significant relationship (fig. 2*A*). We found significant evidence for neutral IBD in *A. piscivorus* ($P = 0.005$) but not in *C. adamanteus* ($P = 0.088$) or *S. miliarius* ($P = 0.054$; fig. 2*B*). We found significant evidence for trait IBD in *A. piscivorus* ($P < 0.001$); again, neither *C. adamanteus* ($P = 0.256$) nor *S. miliarius* ($P = 0.267$) exhibited a significant relationship (fig. 2*C*). To illustrate the relationship between phenotypic differentiation and geographic distance after accounting for neutral genetic differentiation, we compared the residuals from our linear models comparing geographic distance $\sim F_{ST}$ (fig. 2*B*) and venom phenotypic distance $\sim F_{ST}$ (fig. 2*A*). We again found significant evidence for trait IBD in *A. piscivorus* ($P < 0.001$) but not in *C. adamanteus* ($P = 0.552$) or *S. miliarius* ($P = 0.154$; fig. 2*D*).

To ensure that these results were not biased by differences in sample size and/or sampling area across species, we next restricted these analyses to Florida populations where sampling was approximately equivalent across species (fig. 1). We removed five comparisons involving Jekyll and Sapelo islands for *C. adamanteus* and five comparisons involving the continental population for *A. piscivorus*; *S. miliarius* was only sampled in Florida and not reanalyzed. Neutral differentiation was again a significant predictor of phenotypic differentiation in *A. piscivorus* ($P = 0.039, R^2 = 0.392, R = 0.626$) but not *C. adamanteus* ($P = 0.581, R^2 = 0.065, R = 0.255$). We found significant evidence for neutral ($P = 0.035, R^2 = 0.406, R = 0.637$) and trait ($P < 0.001$, $R^2 = 0.793, R = 0.891$) IBD in *A. piscivorus* but not *C. adamanteus* (neutral IBD: $P = 0.927, R^2 = 0.002, R = -0.043$; trait IBD: $P = 0.086$, $R^2 = 0.477, R = 0.690$), consistent with our initial results. We again compared the residuals from our linear models comparing geographic distance $\sim F_{ST}$ and venom phenotypic distance $\sim F_{ST}$ and found significant evidence for trait IBD (after accounting for genetic differentiation) in *A. piscivorus* ($P = 0.004, R^2 = 0.613, R = 0.783$) but not in *C. adamanteus* ($P = 0.097, R^2 = 0.455, R = 0.674$). These concordant results suggest that these analyses were robust to sample size, and the nonsignificant results for *C. adamanteus* and *S. miliarius* are biologically meaningful rather than artifactual.

Although we did not perform all pairwise comparisons to avoid unnecessary, nested pseudoreplication (see Materials and Methods for details), some populations were used in multiple comparisons in the analyses described above. To explicitly address the pseudoreplication that did exist in our data set, we performed Mantel tests to compare the correlation between the venom, geographic distance, and F_{ST} distance matrices for each species independently. Consistent with our previous analyses, we did not find a significant correlation between any distance matrices in *C. adamanteus* ($0.167 \leq P \leq 0.667$) or *S. miliarius* ($0.167 \leq P \leq 1.000$). We found significant

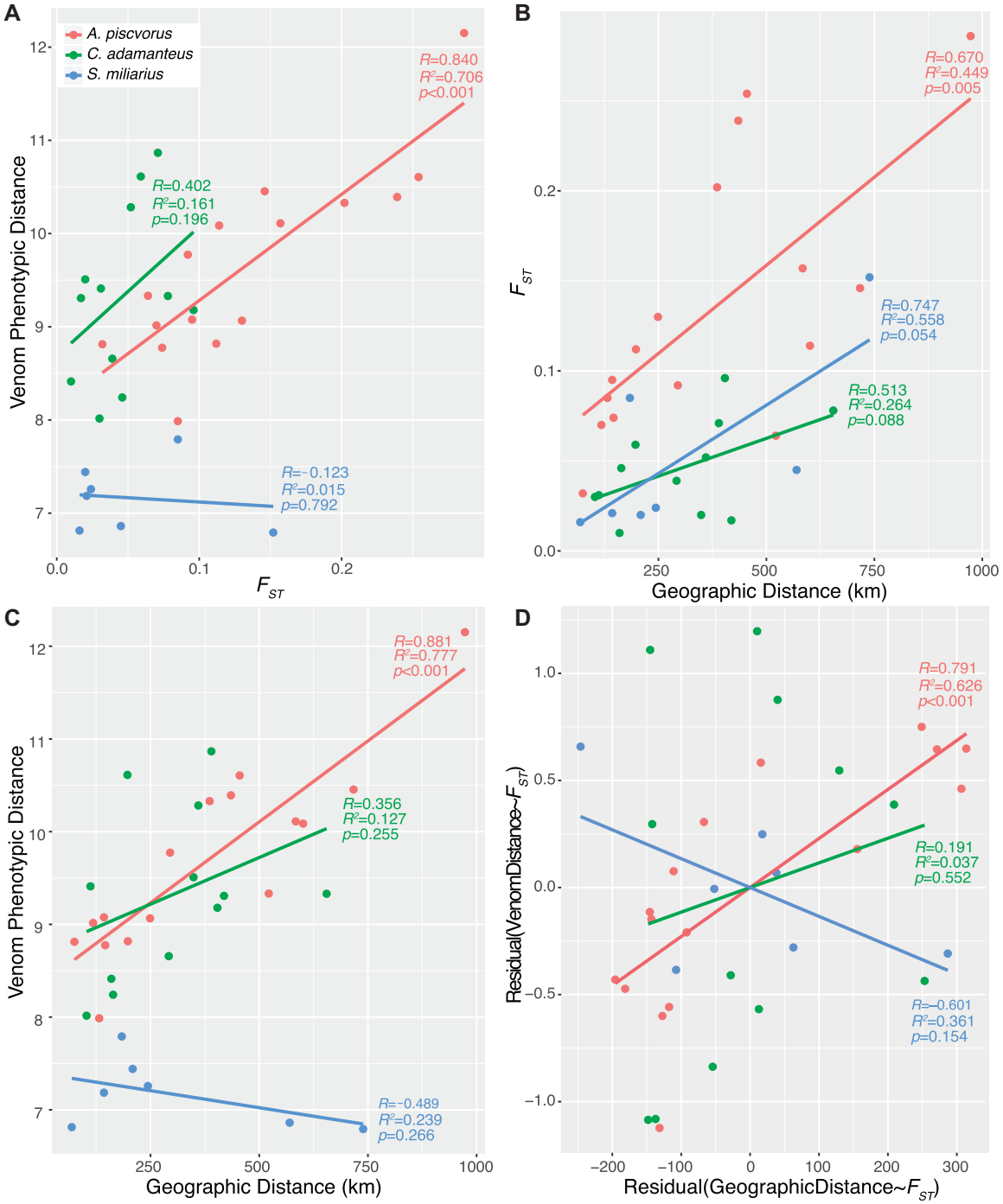

Fig. 2. Comparing phenotypic and neutral genetic differentiation reveals that the migration–selection interaction was biased toward selection in two of the three species. (*A*) Comparing neutral genomic and venom expression differentiation. (*B*) Testing for isolation-by-distance in the neutral genetic data. (*C*) Testing for isolation-by-distance in the venom expression data. F_{ST} was used to estimate neutral genetic distance. (*D*) Comparing the residuals from panels (*A*) (*y* axis) and (*B*) (*x* axis) to illustrate the relationship between venom phenotypic distance and geographic distance after accounting for genomic differentiation (F_{ST}). Venom phenotypic distance was calculated as group dissimilarity in venom expression using the *dist* and *meandist* functions in R and Euclidean distances. Geographic distance was calculated as the straight line distance in kilometers (km) between the mean latitude and longitude of each group. Each point represents a pairwise comparison. *R* is the Pearson's product–moment correlation, R^2 is the coefficient of determination, and *P* values were calculated in simple regression models.

correlations in *A. piscivorus* when comparing the venom and F_{ST} distance matrices ($P = 0.001$) as well as venom and geographic distance ($P = 0.019$); F_{ST} and geographic distance were marginally significant in *A. piscivorus* ($P = 0.061$). We also performed partial Mantel tests to examine the correlation among all three distance matrices for each species independently. Results were concordant with the Mantel tests above; *A. piscivorus* exhibited a significant correlation ($P = 0.018$) where *C. adamanteus* and *S. miliarius* did not ($0.333 \leq P \leq 1.000$).

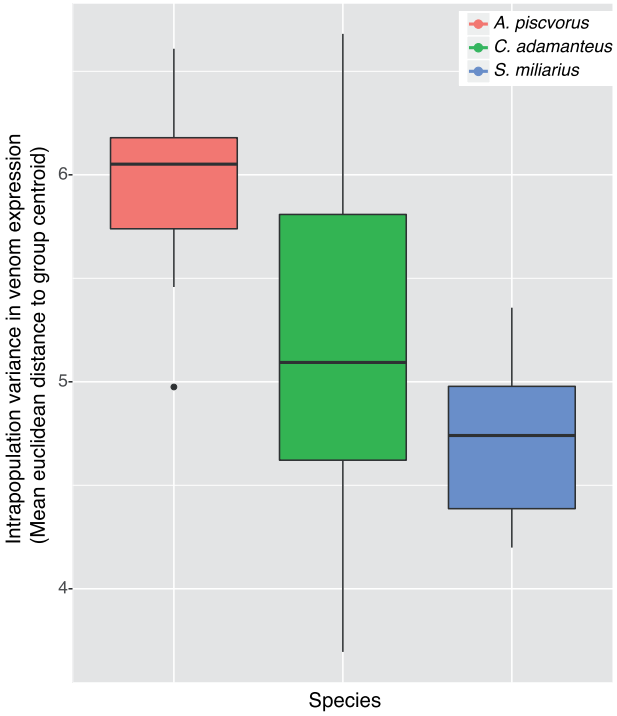

Fig. 3. Intrapopulation variance in venom expression across all three species. Boxplot of within population variance in venom expression for each species. Intrapopulation variance was calculated as the mean Euclidean distance of population members to the population centroid in multivariate space using the *betadisper* function in R. Bars represent the median, boxes extend to the 25% and 75% quantiles, whiskers extend to the largest value $\leq$ 1.5× interquartile range, and points represent outliers exceeding >1.5× interquartile range.

Collectively, these results indicated that selection was the predominant mechanism in the migration–selection balance underlying adaptive venom evolution in *C. adamanteus* and *S. miliarius*, even in the face of high gene flow, whereas gene flow was the driving force in determining/constraining adaptive venom divergence in *A. piscivorus*. Although these results suggest different selective regimes in *S. miliarius*/*C. adamanteus* relative to *A. piscivorus*, the migration–selection balance may still lean toward selection in *A. piscivorus* because gene flow and adaption can influence one another (e.g., reduced immigrant fitness; Garant et al. 2007). Selection and gene flow may also spatially covary, causing more distant subpopulations to experience stronger selection and lower gene flow simultaneously, leading to spurious conclusions regarding the constraining power of gene flow (Garant et al. 2007). Drift could also provide a potential mechanism explaining venom differentiation in *A. piscivorus*. Neutral genetic differentiation was a significant predictor of phenotypic differentiation in *A. piscivorus*, and *A. piscivorus* showed evidence of both neutral and trait IBD, patterns consistent with genetic drift.

Because selection and drift should reduce within population expression variation whereas gene flow is expected to have the opposite effect, we next compared intrapopulation variation in venom expression across all three species (fig. 3) to determine if selective regimes did vary across taxa as suggested above. If the balance leaned toward selection in *C. adamanteus* and *S. miliarius* but toward gene flow in *A. piscivorus*, we would expect to see significantly less intrapopulation variation in venom expression in the former two species relative to *A. piscivorus*. If drift was the mechanism underlying venom differentiation in *A piscivorus*, however, we would expect to see less (or similar levels of) intrapopulation variation in *A piscivorus* relative to *C. adamanteus* and *S. miliarius*. We used an ANOVA to compare within group variances and found a significant difference across species ($P = 0.007$). Both *C. adamanteus* ($P = 0.035$) and *S. miliarius* ($P = 0.002$) possessed significantly less intrapopulation variance than *A. piscivorus* (fig. 3), indicating that 1) the balance leaned toward selection in *C. adamanteus* and *S. miliarius*, and 2) gene flow, rather than drift, was the predominant mechanism determining patterns of venom differentiation in *A. piscivorus*.

Conclusion

The interaction between gene flow and selection is the strongest determinant of whether a beneficial allele increases in frequency within a population (Tigano and Friesen 2016). We argue, therefore, that our results provide evidence that the migration–selection balance was biased toward selection in at least two of the three species in this study, suggesting that the strength of selection, rather than migration rate, had the greatest effect on how quickly advantageous toxin alleles spread across the metapopulation (Slatkin 1976). The spatial scale of adaptation, however, is typically not known for a given system, and trait differences across fine spatial scales can lead to microgeographic adaptation (reviewed in Richardson et al. 2014). Because we found adaptive expression divergence within neutrally defined populations for all three species (i.e., patterns 3 and 4; supplementary figs. S4, S5, S6 Supplementary Material online), future studies need to investigate sampling localities within and beyond neutrally defined population structure as previously suggested (Richardson et al. 2014).

Geographic differences in the relative strength of selection may explain why *S. miliarius* and *C. adamanteus* venoms are frequently diverging in the face of gene flow whereas *A. piscivorus* venoms are only diverging in the absence of gene flow, and these differences in selection strength may be related to their degree of dietary specialization. Recent evidence suggests prey-preference in venomous snakes is genetic (Holding et al. 2016), and, as discussed earlier, the diets of *C. adamanteus* and *S. miliarius* are much more specialized than that of *A. piscivorus* (Kofron 1978; Roth et al. 1999; Vincent et al. 2004; Gibbs and Mackessy 2009; Means 2017). How specialization influences diversity has often been debated, and dispersal has been thought to be a stronger influence on genetic differentiation than specialization (Kelley et al. 2000). Although our sample size was limited to two specialists and a single generalist, our results suggest that selection associated with specialization may be a stronger influence on differentiation than dispersal. Greater specialization may lead to greater diversification rates at micro- and macroevolutionary scales, and extreme spatial and temporal variation in selective pressures can favor generalist phenotypes

where generalists evolve under strong stabilizing selection (Futuyma and Moreno 1988). Our results are consistent with these expectations, suggesting that the equivocal findings of studies examining the role of gene flow in an adaptive context may be explained by ecological specialization theory. Future work in other systems is needed to determine how universally influential specialization is on adaptive diversification and the migration–selection balance.

A trait's genomic architecture can also affect the rate and mechanism of adaptation (Rosenblum et al. 2010; Lourenco et al. 2013; Margres et al. 2017), and simulation studies have suggested that genetic redundancy as well as mutation effects can have a deterministic role on the evolution of the type of genetic architecture under different migration regimes (Yeaman and Whitlock 2011; Yeaman 2015). For example, because divergence in the face of gene flow is more likely with large-effect variants, selection should favor architectures with fewer, larger, and linked variants (Yeaman 2015). As more reference genomes are assembled for snakes (Vonk et al. 2013; Yin et al. 2016; Perry et al. 2018) and other non-models (Murchison et al. 2012; McKenna et al. 2016), we can begin to directly test these hypotheses, and our results suggest that migration, selection, and ecology may all affect the evolution of a particular trait's genomic architecture.

Materials and Methods

Sampling

We collected tissue and/or venom samples from 138 *C. adamanteus*, 127 *S. miliarius*, and 169 *A. piscivorus*. We recorded snout-vent length (SVL), total length (TL), and sex for all live-caught individuals prior to release. Samples were collected under the following permits: Florida Fish and Wildlife Conservation Commission (FWC) LSSC-13-00004 and LSSC-09-0399, Eglin Air Force Base 96 SFS/SFOIRP, Everglades National Park—EVER-2012-SCI-0053, Florida Department of Environmental Protection Division of Recreation and Parks—Permits #04101310 and #03211410, St Vincent National Wildlife Refuge—Permit #41650-2012-08, Mississippi Department of Wildlife, Fisheries, and Parks Salvage Permit, and Sapelo Island NERR Research Projects collaboration. The above procedures were approved by the Florida State University Institutional Animal Care and Use Committee (IACUC) under protocols #0924 and #1333.

Probe Design, Library Preparation, and Sequencing

We sequenced 138 *C. adamanteus*, 95 *S. miliarius*, and 142 *A. piscivorus*. Target capture probes for 348 anchor (Lemmon et al. 2012; Ruane et al. 2015), 240 long anonymous (~2,000 bp), and 829 short anonymous (~250 bp) loci were designed as previously described (Margres et al. 2017; Margres et al. 2017). Samples were sequenced as previously described (Margres et al. 2017) through the Center for Anchored Phylogenomics at Florida State University (www.anchoredphylogeny.com). Sequencing was performed in the Translational Science Laboratory in the College of Medicine at Florida State University, and all samples were sequenced PE150, PE200, and/or PE250 on an Illumina HiSeq2500 as previously described (Margres et al. 2017).

Alignments and Variant Calling

Reference sequences for all anchored, short anonymous, and long anonymous loci to be used in alignments for variant calling were generated as previously described (Margres et al. 2017). Raw reads were merged with PEAR (Zhang et al. 2014) and alignments generated using the BWA-MEM algorithm (Li and Durbin 2009). We used merged and unmerged reads for assembly. Variant calling was performed in GATK (McKenna et al. 2010; DePristo et al. 2011) as previously described (Margres et al. 2017).

Identifying Genetic Structure

We used a discriminant analysis of principal components, or DAPC (Jombart et al. 2010), in the *adegenet* package (Jombart 2008) in R to identify distinct genetic clusters for each species independently. This approach uses discriminant functions to maximize variation between and minimize variation within different genetic clusters. The best number of clusters (i.e., k) was identified by using a clustering algorithm that maximizes variation between groups; Bayesian Information Criterion (BIC) was used to compare models for $k = 1$–20, and all principal components were retained during cluster identification. Following cluster identification, we used the *dapc* function (Jombart 2008) to describe the genetic clusters identified in the previous step. To avoid overfitting the data, we used the *a.score* from the *adegenet* package (Jombart 2008) to select the optimal number of principal components to retain during the DAPC as suggested by the tutorial. The *a.score* is the difference between the proportion of successful reassignment and random values. All discriminant functions were retained. We then estimated Weir and Cockerham's mean and weighted F_{ST} (Weir and Cockerham 1984) across the identified genetic clusters using vcftools (Danecek et al. 2011).

Population-Phylogenetic Inference

To complement our DAPC runs, we inferred unrooted phylogenies for each of the three species using SVDquartets (Chifman and Kubatko 2014) in PAUP* v4.0a157 (Swofford 1998). SVDquartets uses SNPs to infer relationships among quartets of taxa under a coalescent model in which each site is assumed to have its own genealogy; SVDquartets does not necessitate independence among sites (i.e., multiple SNPs in linkage may be used). By estimating quartet genealogies for each site, the sample-wide phylogeny may be estimated by assembling the resultant quartets. We produced multiple sequence alignments in fasta format using PGDspider v2.1.1.2 (Lischer and Excoffier 2012) and custom scripts for each species. When converting from variant call to fasta format, PGDspider produces two concatenated sequences per sample: one generated from the concatenation of the first allele across all sites, and one from the second allele across all sites. We produced the input sequences for SVDquartets by concatenating these two resultant sequences for each individual. For each species, all quartets were estimated under the multispecies coalescent model (expecting matrix-rank 10),

and these quartets were assembled using the QFM algorithm. Confidence in tree topology was quantified through nonparametric bootstrapping. A consensus tree was produced by summarizing across bootstrapped trees using the SumTrees program as implemented in DendroPy v4.3.0 (Sukumaran and Holder 2010) using –force-unrooted and –min-clade-freq = 0.25. Consensus trees were visualized using FigTree v1.4.3 (Rambaut 2012).

Estimating Effective Migration Surfaces

We used the program EEMS (Petkova et al. 2016) to estimate and project spatially variable migration rates across the landscape for each species independently. Briefly, EEMS models the effective migration rate as the rate at which genetic dissimilarity decays under a population genetic stepping stone model. Under this model, individuals may migrate among adjacent demes, and the rates at which these individuals migrate can spatially vary. To approximate continuous population structure, a dense regular grid is superimposed across the landscape, and expected genetic dissimilarities across this landscape are modeled using resistance distance, thus integrating across all possible migration routes among demes (McRae 2006). We used QGIS 2.0.1—Dufour (Team 2009) to generate the bounding polygons for each species in which deme grids were overlain. Briefly, shapefiles for Alabama, Florida, Georgia, Mississippi, and South Carolina were downloaded from the United States Census Bureau (Bureau 2017); 30-km buffers were calculated around each state boundary and merged with the state polygon. These resultant polygons were then manually reduced to contain only sampled locations and coastlines (i.e., unsampled portions of the state were excluded), and the outer coordinates for these shapefiles provided the bounding polygon for the EEMS analyses. We converted the SNP data to PLINK format (Purcell et al. 2007) and then calculated the pairwise difference matrix using the bed2diffs function in EEMS. Missing genotypes were not imputed. Following the authors recommendations, we used EEMS to estimate migration surfaces for two deme sizes (750 and 1,000), and the final results were obtained by averaging across runs (Petkova et al. 2016). For each deme size, we conducted two runs. For each run, the MCMC was run for ten million generations, sampling every 10,000 generations with a burn-in of one million generations. The posterior for each chain, therefore, was comprised of 1,000 samples with a total of 2,000 samples per deme size. MCMCs were visually assessed for convergence (supplementary fig. S7, Supplementary Material online). Effective migration surfaces and respective posterior probabilities were visualized using the reemsplots2 R package (R Development Core Team 2013). Here, the contour plot was produced by sampling from the posterior distribution of migration rates and interpolating rates between grid points. Effective migration rates are shown as migrants per generation on a log scale relative to the overall migration rate across the landscape (Petkova et al. 2016). Mean, untransformed effective migration rates for each DAPC genetic cluster were calculated by extracting the value at each individual sampling location and averaging across all individuals/DAPC genetic cluster. Effective migration rates represent the number of migrants per generation being exchanged between the specific DAPC cluster and neighboring demes.

Venom Statistical Analyses

We collected venom from 91 *C. adamanteus*, 127 *S. miliarius*, and 169 *A. piscivorus*. To increase sample sizes for the expression analyses, individuals not included in the sequence-based analyses but originating from the same populations were included in RP-HPLC-based analyses. Twenty-five rRP-HPLC peaks per *C. adamanteus* venom sample, 28 peaks per *S. miliarius* venom sample, and 38 peaks per *A. piscivorus* venom sample were quantified as previously described (Margres et al. 2014; Margres et al. 2015; Wray et al. 2015). We used the ilr transformation (Egozcue et al. 2003) to transform the data using the *robCompositions* package (Templ et al. 2011) in R prior to statistical analyses (Filzmoser et al. 2009). We used the multiplicative replacement strategy (Martin-Fernandez et al. 2003) implemented in the R package *zCompositions* assuming a detection threshold of 0.01% (the smallest measured value) to resolve the issue of zeros. We used the *adonis* function from the *vegan* package (Oksanen et al. 2007) in R and Euclidean distances to perform a permutational or nonparametric MANOVA (McArdle and Anderson 2001) on the ilr-transformed data to test for significant protein expression differentiation as previously described (Margres et al. 2015); we chose to use the Euclidean distance because Euclidean distance on the real space is equivalent to the Aitchison distance in compositional space. Results were visualized using the *betadisper* function (i.e., multivariate homogeneity of groups dispersions).

Because ontogenetic shifts in venom expression are common among pit vipers (Mackessy 1988; Durban et al. 2013; Margres et al. 2015; Wray et al. 2015; Rokyta et al. 2017), we separated individuals into age classes to test for ontogenetic expression variation in these species. *Crotalus adamanteus* $<$102 cm SVL were classified as juveniles, and *C. adamanteus* $\geq$ 102 cm were classified as adults based on previous work (Waldron et al. 2013; Margres et al. 2015). *Sistrurus miliarius* $<$28 cm SVL were classified as juveniles, and individuals $\geq$ 28 cm were classified as adults (Smiley-Walters et al. 2017). *Agkistrodon piscivorus* $<$45 cm were classified as juveniles, and individuals $\geq$ 45 cm were classified as adults (Burkett 1966). Population designations were consistent with population structure analyses. Using this adult-only data, we used the *dist* and *meandist* functions in R to calculate between group dissimilarity in venom expression using Euclidean distances and the ilr-transformed data. We performed all pairwise comparisons for 1) the identified DAPC clusters, and 2) the sampling localities within each DAPC cluster. For example, in *C. adamanteus*, we performed 1) all pairwise comparisons for the three DAPC genetic clusters (East, West, Jekyll; supplementary fig. S4*A*, Supplementary Material online), 2) all pairwise comparisons of the four sampling localities present within the East DAPC genetic cluster (supplementary fig. S4*B*, Supplementary Material online), and 3) all pairwise comparisons of the three sampling localities present within the West DAPC genetic cluster (supplementary fig. S4*C*, Supplementary Material online). We never compared, however, the West1

and Everglades sampling localities in supplementary figure S4D, Supplementary Material online, to avoid unnecessary, nested pseudoreplication as these sites were already compared when looking across DAPC clusters (i.e., East vs. West). To explicitly address the pseudoreplication that did exist in our data set, we performed Mantel and partial Mantel tests to compare the correlation between the venom, geographic distance, and F_{ST} distance matrices using the *vegan* package (Oksanen et al. 2007) in R.

Supplementary Material

Supplementary data are available at *Molecular Biology and Evolution* online.

Acknowledgments

This work was supported by the National Science Foundation under DEB 1145987 to A.R.L., E.M.L., and D.R.R. as well as through the National Science Foundation Graduate Research Fellowship Program under Grant No. 1449440 to M.J.W. and D.R.R. Any opinions, findings, and conclusions or recommendations expressed in this material are those of the authors and do not necessarily reflect the views of the National Science Foundation. The authors thank Kimberley Andrews and Joseph Colbert at the Jekyll Island Authority's Georgia Sea Turtle Center, Jim Lee and The Nature Conservancy at Camp Shelby Military Base, Karen Relish with Fakahatchee Strand State Preserve, Robert Dye and Myakka River State Park, Jim Mendenhall, Mike Martin, Brice Noonan, and Lora Smith and Jennifer Howze at the Joseph W. Jones Ecological Research Center at Ichuaway for help in acquiring venom and tissue samples. The authors thank Megan Lamb, Ethan Bourque, and Rebecca Bernard with the Florida DEP and Apalachicola River NERR, Bradley Smith and the St Vincent NWR, Dorset Hurley and Doug Samson at the Sapelo Island NERR, Brett Williams and the Department of the Air Force, and Peter Krulder, Carl Calhoun, and Rick Coosey at Caladesi Island State Park for access to field sites. We thank Michelle Kortyna and Ameer Jalal at FSU's Center for Anchored Phylogenomics for assistance with hybrid enrichment data collection and analysis. Reads were deposited in the NCBI Sequence Read Archive under accession SRP011323.

References

Bert T. 1986. Speciation in western Atlantic stone crabs (genus *Menippe*): the role of geological processes and climatic events in the formation and distribution of species. *Mar Biol*. 93:157–170.

Blanquart F, Kaltz O, Nuismer S, Gandon S. 2013. A practical guide to measuring local adaptation. *Ecol Lett*. 16(9):1195–1205.

Boldrini-França J, Corrêa-Netto C, Silva MMS, Rodrigues RS, Torre PDL, Pérez A, Soares AM, Zingali RB, Nogueira RA, Rodrigues VM, et al. 2010. Snake venomics and antivenomics of *Crotalus durissus* subspecies from Brazil: assessment of geographic variation and its implication on snakebite management. *J Proteomics*. 73(9):1758–1776.

Bulmer M. 1972. The genetic variability of polygenic characters under optimizing selection, mutation, and drift. *Genet Res*. 19(01):17–25.

Burkett R. 1966. Natural history of cottonmouth moccasin, *Agkistrodon piscivorus* (Reptilia) [master's thesis]. Lawrence, KS: University of Kansas.

Calvete JJ, Sanz L, Cid P, de la Torre P, Flores-Díaz M, Dos Santos MC, Borges A, Bremo A, Angulo Y, Lomonte B, et al. 2010. Snake venomics of the central American rattlesnake *Crotalus simus* and the south American *Crotalus durissus* complex points to neurotoxicity as an adaptive paedomorphic trend along *Crotalus* dispersal in South America. *J Proteome Res*. 9(1):528–544.

Casewell NR, Huttley GA, Wüster W. 2012. Dynamic evolution of venom proteins in squamate reptiles. *Nat Commun*. 3:1066.

Casewell NR, Wagstaff SC, Harrison RA, Renjifo C, Wüster W. 2011. Domain loss facilitates accelerated evolution and neofunctionalization of duplicate snake venom metalloproteinase toxin genes. *Mol Biol Evol*. 28(9):2637–2649.

Charlesworth B, Lande R, Slatkin M. 1982. A neo-Darwinian commentary on macroevolution. *Evolution* 36(3):474–498.

Chifman J, Kubatko L. 2014. Quartet inference from SNP data under the coalescent. *Bioinformatics* 30(23):3317–3324.

Colosimo P, Hosemann K, Balabhadra S, Villarreal G, Dickson M, Grimwood J, Schmutz J, Myers R, Schluter D, Kingsley D. 2005. Widespread parallel evolution in sticklebacks by repeated fixation of ectodysplasin alleles. *Science* 307(5717):1928–1933.

Daltry JC, Wüster W, Thorpe RS. 1996. Diet and snake venom evolution. *Nature* 379(6565):537–540.

Danecek P, Auton A, Abecasis G, Albers CA, Banks E, DePristo MA, Handsaker RE, Lunter G, Marth GT, Sherry ST, et al. 2011. The variant call format and VCFtools. *Bioinformatics* 27(15):2156–2158.

DePristo M, Banks E, Poplin R, Garimella K, Maguire J, Hartl C, Philippakis A, del Angel G, Rivas M, Hanna M, et al. 2011. A framework for variation discovery and genotyping using next-generation DNA sequencing data. *Nat Genet*. 43(5):491–498.

Devictor V, Clavel J, Julliard R, Lavergne S, Mouillot D, Thuiller W, Venail P, Villeger S, Mouquet N. 2010. Defining and measuring ecological specialization. *J Appl Ecol*. 47(1):15–25.

Durban J, Perez A, Sanz L, Gomez A, Bonilla F, Rodriguez S, Chacon D, Sasa M, Angulo Y, Gutierrez J, et al. 2013. Integrated "omics" profiling indicates that mirnas are modulators of the ontogenetic venom composition shift in the central American rattlesnake, *Crotalus simus simus*. *BMC Genomics* 14(1):234.

Egozcue JJ, Pawlowsky-Glahn V, Mateu-Figueras G, Barceló-Vidal C. 2003. Isometric logratio transformations for compositional data analysis. *Math Geol*. 35(3):279–300.

Ehrlich P, Raven P. 1969. Differentiation of populations. *Science* 165(3899):1228–1232.

Endler J. 1977. Geographic variation, speciation, and clines. Princeton (NJ): Princeton University Press.

Felsenstein J. 1977. Multivariate normal genetic model with a finite number of loci. In Pollak E, Kempthorne O, Bailey T Jr, editors. Proceedings of the International Conference on Quantitative Genetics. Ames (IA): Iowa State University Press. p. 227–246.

Filzmoser P, Hron K, Reimann C. 2009. Principal component analysis of compositional data with outliers. *Environmetrics* 20(6):621–632.

Fitzpatrick S, Gerberich J, Kronenberger J, Angeloni L, Funk W. 2015. Locally adapted traits maintained in the face of high gene flow. *Ecol Lett*. 18(1):37–47.

Futuyma D, Moreno G. 1988. The evolution of ecological specialization. *Annu Rev Ecol Syst*. 19(1):207–233.

Gandon S, Nuismer S. 2009. Interactions between genetic drift, gene flow, and selection mosaics drive parasite local adaptation. *Am Nat*. 173(2):212–224.

Garant D, Forde SE, Hendry AP. 2007. The multifarious effects of dispersal and gene flow on contemporary adaptation. *Funct Ecol*. 21(3):434–443.

Garcia-Ramos G, Kirkpatrick M. 1997. Genetic models of adaptation and gene flow in peripheral populations. *Evolution* 51(1):21–28.

Gibbs HL, Mackessy SP. 2009. Functional basis of a molecular adaptation: prey-specific toxic effects of venom from *Sistrurus* rattlesnakes. *Toxicon* 53(6):672–679.

Gomulkiewicz R, Drown D, Dybdahl M, Godsoe W, Nuismer S, Pepin K, Ridenhour B, Smith C, Yoder J. 2007. Dos and don'ts of testing the geographic mosaic theory of coevolution. *Heredity* 98(5):249–258.
Groot A, Classen A, Inglis O, Blanco C, Lopez J, Vargas A, Schal C, Heckel D, Schofl G. 2011. Genetic differentiation across North America in the generalist moth *Heliothis virescens* and the specialist *H. subflexa*. *Mol Ecol*. 20(13):2676–2692.
Holding M, Biardi J, Gibbs H. 2016. Coevolution of venom function and venom resistance in a rattlesnake predator and its squirrel prey. *Proc R Soc B*. 283(1829):20152841.
Holding M, Denton R, Gibbs H. 2016. Fixed prey cue preferences among dusky pigmy rattlesnakes (*Sistrurus miliarius barbouri*) raised on different long-term diets. *Evol Ecol*. 30(1):1–7.
Jombart T. 2008. adegenet: a R package for the multivariate analysis of genetic markers. *Bioinformatics* 24(11):1403–1405.
Jombart T, Devillard S, Balloux F. 2010. Discriminant analysis of principal components: a new method for the analysis of genetically structured populations. *BMC Genet*. 11(1):94.
Kelley S, Farrell B, Mitton J. 2000. Effects of specialization on genetic differentiation in sister species of bark bettles. *Heredity* 84(2):218–227.
Kofron C. 1978. Foods and habitats of aquatic snakes (Reptilia, Serpentes) in a Louisiana swamp. *J Herpetol*. 12(4):543–554.
Lemmon A, Emme S, Lemmon E. 2012. Anchored hybrid enrichment for massively high-throughput phylogenomics. *Syst Biol*. 61(5):727–744.
Lenormand T. 2002. Gene flow and the limits to natural selection. *Trends Ecol Evol*. 17(4):183–189.
Li H, Durbin R. 2009. Fast and accurate short read alignment with Burrows-Wheeler Transform. *Bioinformatics* 25(14):1754–1760.
Linnen C, Poh Y, Peterson B, Barrett R, Larson J, Jensen J, Hoekstra H. 2013. Adaptive evolution of multiple traits though multiple mutations at a single gene. *Science* 339(6125):1312–1316.
Linnen CR, Kingsley EP, Jensen JD, Hoekstra HE. 2009. On the origin and spread of an adaptive allele in deer mice. *Science* 325(5944): 1095–1098.
Lischer H, Excoffier L. 2012. Pgdspider: an automated data conversion tool for connecting population genetics and genomics programs. *Bioinformatics* 28(2):298–299.
Lourenco J, Glemin S, Galtier N. 2013. The rate of molecular adaptation in a changing environment. *Mol Biol Evol*. 30(6):1292–1301.
Mackessy SP. 1988. Venom ontogeny in the Pacific rattlesnakes *Crotalus viridis helleri* and *C. v. oreganus*. *Copeia* 1988(1):92–101.
Margres M, Aronow K, Loyacano J, Rokyta D. 2013. The venom-gland transcriptome of the eastern coral snake (*Micrurus fulvius*) reveals high venom complexity in the intragenomic evolution of venoms. *BMC Genomics* 14(1):531.
Margres M, Bigelow A, Lemmon E, Lemmon A, Rokyta D. 2017. Selection to increase expression, not sequence diversity, precedes gene family origin and expansion in rattlesnake venom. *Genetics* 206(3):1569–1580.
Margres M, McGivern J, Seavy M, Wray K, Facente J, Rokyta D. 2015. Contrasting modes and tempos of venom expression evolution in two snake species. *Genetics* 199(1):165–176.
Margres M, McGivern J, Wray K, Seavy M, Calvin K, Rokyta D. 2014. Linking the transcriptome and proteome to characterize the venom of the eastern diamondback rattlesnake (*Crotalus adamanteus*). *J Proteomics*. 96:145–158.
Margres M, Hassinger A, Ward M, McGivern J, Lemmon E, Lemmon A, Rokyta D. 2017. Quantity, not quality: rapid adaptation in a polygenic trait proceeded exclusively through expression differentiation. *Mol Biol Evol*. 34(12):3099–3110.
Margres M, Wray K, Seavy M, McGivern J, Herrera N, Rokyta D. 2016. Expression differentiation is constrained to low-expression proteins over ecological timescales. *Genetics* 202(1):273–283.
Margres M, Seavy M, McGivern J, Sanader D, Rokyta D. 2015. Phenotypic integration in the feeding system of the eastern diamondback rattlesnake (*Crotalus adamanteus*). *Mol Ecol*. 24(13):3405–3420.
Martin C, Wainwright P. 2013. Multiple fitness peaks on the adaptive landscape drive adaptive radiation in the wild. *Science* 339(6116):208–211.
Martin-Fernandez J, Barcelo-Vidal C, Pawlowsky-Glahn V. 2003. Dealing with zeros and missing values in compositional data sets using nonparametric imputation. *Math Geol*. 35(3):253–278.
McArdle B, Anderson M. 2001. Fitting multivariate models to community data: a comment on distance-based redundancy analysis. *Ecology* 82(1):290–297.
McKenna A, Hanna M, Banks E, Sivachenko A, Cibulskis K, Kernytsky A, Garimella K, Altshuler D, Gabriel S, Daly M, et al. 2010. The Genome Analysis Toolkit: a MapReduce framework for analyzing next-generation DNA sequencing data. *Genome Res*. 20(9):1297–1303.
McKenna D, Scully E, Pauchet Y, Hoover K, Kirsch R, Geib S, Mitchell R, Waterhouse R, Ahn S, et al. 2016. Genome of the Asian longhorned beetle (*Anoplophora glabripennis*), a globally significant invasive species, reveals key functional and evolutionary innovations at the beetle-plant interface. *Genome Biol*. 17(1):227.
McRae B. 2006. Isolation by resistance. *Evolution* 60(8):1551–1561.
Means D. 2017. Diamonds in the rough, natural history of the eastern diamondback rattlesnake. Tallahassee (FL): Tall Timbers Press.
Muir A, Biek R, Thomas R, Mable B. 2014. Local adaptation with high gene flow: temperature parameters drive adaptation to altitude in the common frog (*Rana temporaria*). *Mol Ecol*. 23(3): 561–574.
Murchison EP, Schulz-Trieglaff OB, Ning Z, Alexandrov LB, Bauer MJ, Fu B, Hims M, Ding Z, Ivakhno S, Stewart C, et al. 2012. Genome sequencing and analysis of the Tasmanian devil and its transmissible cancer. *Cell* 148(4):780–791.
Nuismer S, Gandon S. 2008. Moving beyond common-garden and transplant designs: insight into the causes of local adaptation in species interactions. *Am Nat*. 171(5):658–668.
Oksanen J, Blanchet F, Kindt R, Legendre P, Minchin P, O'Hara R, Simpson G, Solymos P, Henry M, Stevens H, Wagner H. 2007. The vegan package. *Commun Ecol Package*. 631–637.
Packer L, Zayed A, Grixti J, Ruz L, Owen R, Vivallo F, Toro H. 2005. Conservation genetics of potentially endangered mutualisms: reduced levels of genetic variation in specialist versus generalist bees. *Conserv Genet*. 19(1):195–202.
Perry B, Card D, McGlothlin J, Pasquesi G, Adams R, Schield D, Hales N, Corbin A, Demuth J, Hoffmann F, et al. 2018. Molecular adaptations for sensing and securing prey and insight into amniote genome diversity from the garter snake genome. *Genome Biol Evol*. 10(8):2110–2129.
Petkova D, Novembre J, Stephens M. 2016. Visualizing spatial population structure with estimated effective migration surfaces. *Nat Genet*. 48(1):94–100.
Pfeifer S, Laurent S, Sousa V, Linnen C, Foll M, Excoffier L, Hoekstra H, Jensen J. 2018. The evolutionary history of Nebraska deer mice: local adaptation in the face of strong gene flow. *Mol Biol Evol*. 35(4):792–806.
Purcell S, Neale B, Todd-Brown K, Thomas L, Ferreira M, Bender D, Maller J, Sklar P, de Bakker P, Daly M, et al. 2007. PLINK: a tool set for whole-genome association and population-based linkage analysis. *Am J Hum Genet*. 81(3):559–575.
QGIS Development Team. 2009. QGIS geographic information system. Open Source Geospatial Foundation.
R Development Core Team. 2013. R: a language and environment for statistical computing.
Rambaut A. 2012. FigTree v1.4. Molecular evolution, phylogenetic, and epidemiology. Edinburgh (United Kingdom): University of Edinburgh, Institute of Evolutionary Biology.
Richardson J, Urban M, Bolnick D, Skelly D. 2014. Microgeographic adaptation and the spatial scale of evolution. *Trends Ecol Evol*. 29(3):165–176.
Rokyta D, Margres M, Ward M, Sanchez E. 2017. The genetics of venom ontogeny in the eastern diamondback rattlesnake (*Crotalus adamanteus*). *PeerJ* page 5:e3249.
Rosenblum E, Rompler H, Schoneberg T, Hoekstra H. 2010. Molecular and functional basis of phenotypic convergence in white lizards at White Sands. *Proc Natl Acad Sci U S A*. 107(5):2113–2117.

Roth ED, May PG, Farrell TM. 1999. Pigmy rattlesnakes use frog-derived chemical cues to select foraging sites. *Copeia* 1999(3):772–774.
Ruane S, Raxworthy C, Lemmon A, Lemmon E, Burbrink F. 2015. Comparing species tree estimation with large anchored phylogenomic and small Sanger-sequenced molecular datasets: an empirical study on Malagasy pseudoxyrhophiine snakes. *BMC Evol Biol*. 15(1):1.
Sánchez EE, Galán JA, Powell RL, Reyes SR, Soto JG, Russell WK, Russell DH, Pérez JC. 2005. Disintegrin, hemorrhagic, and proteolytic activities of Mojave rattlesnake, *Crotalus scutulatus scutulatus* venoms lacking Mojave toxin. *Comp Biochem Physiol C*. 141:124–132.
Savolainen O, Lascoux M, Merila J. 2013. Ecological genomics of local adaptation. *Nat Rev Genet*. 14(11):807–820.
Sexton J, Hangartner S, Hoffmann A. 2014. Genetic isolation by environment or distance: which pattern of gene flow is most common? *Evolution* 68(1):1–15.
Slatkin M. 1976. The rate of spread of an advantageous allele in a subdivided population. In Population genetics and ecology. Elsevier. p. 767–780.
Slatkin M. 1987. Gene flow and the geographic structure of natural populations. *Science* 236(4803):787–792.
Smiley-Walters S, Farrell T, Gibbs H. 2017. Evaluating local adaptation of a complex phenotype: reciprocal tests of pigmy rattlesnake venoms on treefrog prey. *Oecologia* 184(4):739–748.
Sukumaran J, Holder M. 2010. Dendropy: a python library for phylogenetic computing. *Bioinformatics* 26(12):1569–1571.
Swofford DL. 1998. Phylogenetic Analysis Using Parsimony* (PAUP*), version 4.0. Sunderland (MA): Sinauer Associates.
Templ M, Hron K, Filzmoser P. 2011. Compositional data analysis. Theory and applications, Chichester (United Kingdom): John Wiley & Sons.
Tigano A, Friesen V. 2016. Genomics of local adaptation with gene flow. *Mol Ecol*. 25(10):2144–2164.
United States Census Bureau. 2017. Cartographic boundary shapefiles.
Vincent S, Herrel A, Irschick D. 2004. Sexual dimorphism in head shape and diet in the cottonmouth snake (*Agkistrodon piscivorus*). *J Zool Lond*. 264(1):53–59.
Vonk F, Casewell N, Henkel C, Heimberg A, Jansen H, McCleary R, Kerkkamp H, Vos R, Guerreiro I, Calvete J, et al. 2013. The king cobra genome reveals dynamic gene evolution and adaptation in the snake venom system. *Proc Natl Acad Sci U S A*. 110(51):20651–20656.
Waldron JL, Welch SM, Bennett SH, Kalinowsky WG, Mousseau TA. 2013. Life history constraints contribute to the vulnerability of a declining North American rattlesnake. *Biol Conserv*. 159:530–538.
Weir BS, Cockerham CC. 1984. Estimating *f*-statistics for the analysis of population structure. *Evolution* 38(6):1358–1370.
Whitehead A, Crawford D. 2006. Neutral and adaptive variation in gene expression. *Proc Natl Acad Sci U S A*. 103(14):5425–5430.
Wray K, Margres M, Seavy M, Rokyta D. 2015. Early significant ontogenetic changes in snake venoms. *Toxicon* 96:74–81.
Yeaman S. 2015. Local adaptation by alleles of small effect. *Am Nat*. 186(S1):S74–S89.
Yeaman S, Whitlock M. 2011. The genetic architecture of adaptation under migration-selection balance. *Evolution* 65(7):1897–1911.
Yin W, Wang Z, Li Q, Lian J, Zhou Y, Lu B, Jin L, Qiu P, Zhang P, Zhu W, et al. 2016. Evolutionary trajectories of snake genes and genomes revealed by comparative analyses of five-pacer viper. *Nat Commun*. 7:13107.
Zhang J, Kobert K, Flouri T, Stamatakis A. 2014. PEAR: a fast and accurate Illumina Paired-End reAd mergeR. *Bioinformatics* 30(5):614–620.